Constraints on Mantle Convection From Seismic Tomography

Hrafnkell Kárason and Rob D. van der Hilst

Department of Earth, Atmospheric, and Planetary Sciences, Massachusetts Institute of Technology, Cambridge, Massachusetts

Since the advent of global seismic tomography some 25 years ago, advances in technology, seismological theory, and data acquisition have allowed spectacular progress in our ability to image seismic heterogeneity in Earth's mantle. Using examples from some recently published tomographic models, we briefly review some concepts of seismic tomography, such as parameterization, and summarize how this class of imaging has contributed to our knowledge of the scale of mantle convection. With the presently available data seismologists can map the subduction of former oceanic lithosphere beneath most island arcs. Tomographic imaging has revealed that many slabs extend below the deepest earthquakes of the Wadati-Benioff zones and sink deep into the lower mantle, although intense deformation of flow trajectories has been detected in the upper mantle transition zone beneath several convergent margins (in particular in the western Pacific). We illustrate this with examples of our recent 3-dimensional model for mantle *P*-wavespeed, which is inferred from arrival time data of *P*, *pP*, *PKP*, and P_{diff} waves. In combination with constraints from computational geodynamics the seismic images render mantle stratification at 660 km depth unlikely and show that surface plate motions are tied to large scale convective circulation. However, the ultimate fate of the slabs that penetrate into the lower mantle is still enigmatic and in some recent tomographic models the subduction related heterogeneity pattern vanishes at very large depth (2000 km or so). These observations have inspired models for mantle convection that have the potential for reconciling geophysical views and geochemical constraints, but much work remains to be done to establish the detailed pattern of mantle flow.

INTRODUCTION

The relative motion of lithospheric plates at the surface of the Earth, which is directly related to natural hazards such as earthquakes and volcanoes and can cause long-term variations in climate, is the surface expression of slow, large scale deformation of rock in the deep interior of our planet. On a time scale of millions of years the mantle silicates flow in a process known as 'mantle convection', but on short time scales mantle material behaves as a solid. This viscoelastic behavior allows the propagation of longitudinal (*P*) and transverse (*S*) seismic waves, which speed up in "cold" downwellings and slow down in "hot" upwellings so that recordings of these waves can be used for the mapping of mantle flow. Our objective here is not to provide a rigorous review of seismic tomography but to highlight developments in seismic imaging pertinent to the scope of this special volume.

The History and Dynamics of Global Plate Motions
Geophysical Monograph 121
Copyright 2000 by the American Geophysical Union

In the past half century, the scale of mantle convection, which relates critically to compositional stratification and the thermal and chemical evolution of our planet, has been one of the big puzzles in Earth Sciences. A major challenge has been to evaluate and reconcile the range of observations and constraints provided by different scientific disciplines [cf. *Albarède and Van der Hilst*, 1999]. Earth's heat budget (the balance between heat production and heat loss) and geochemical analyses of ocean floor basalts suggest that distinct mantle reservoirs have retained their identity for 2 billion years or more. One reservoir boundary is typically placed at 660 km depth, that is, between the upper and lower mantle. Seismic imaging and computational geodynamics indicate, however, that this interface is not an effective barrier to mantle flow and suggest that convective circulation occurs at a larger scale.

THREE DECADES OF SEISMIC TOMOGRAPHY

Since the pioneering studies in the mid 1970's [see, for instance, *Julian and Sengupta*, 1973; *Sengupta and Toksöz*, 1976; *Aki et al.*, 1977; *Dziewonski et al.*, 1977; *contributions to the 1975 AGU Fall Meeting* (*EOS Trans. of the Am. Geophys. Un.*, 56, 393-396, 1975)], advances in technology (e.g., three to five orders of magnitude increase in computer processing speed, mass storage, and memory), inverse theory, and data quality and volume have vastly improved the tomographic imaging of Earth's deep interior structure. In a parallel development, our understanding of the images has improved dramatically because spectacular advances in computational geodynamics have facilitated the integration of the geological constraints on past plate motion at Earth's surface and the results of experimental and theoretical mineral physics with the snapshots of convection provided by seismic imaging.

Different inversion strategies

For the imaging of global structure two methods have become popular, each with specific benefits and shortcomings. The first represents lateral variations in seismic properties by superposition of global basis functions, such as spherical harmonics. This class of tomography [for reviews see *Woodhouse and Dziewonski*, 1989; *Romanowicz*, 1991; *Montagner*, 1994; *Ritzwoller and Lavely*, 1995; *Ekström*, this volume; *Mégnin and Romanowicz*, this volume] is attractive for imaging structure at a long wavelength, λ, because the number of model parameters, which scales as l^2 — with harmonic degree l inversely proportional to wavelength ($\lambda = 2\pi r/l$), is then small enough to resolve the coefficients by direct inversion of carefully selected and processed waveform data. Plate 1a depicts long wavelength variations in shear wavespeed at 1300 km depth according to the l=12 model of Su et al. [1994]; at this depth, the (half wavelength) resolution is 1350 km.

The large number of global basis functions required to describe structure at length scales of several hundred km or less, such as slabs of subducted lithosphere in the upper mantle, would prohibit direct inversion. Moreover, the coefficients can no longer be determined accurately owing to uneven data coverage on the relevant length scales, and artifacts can be introduced in regions of poor coverage [*Boschi and Dziewonski*, 1999]. It then becomes attractive to represent wavespeed variations by local basis functions, such as non-overlapping constant-slowness volumes (e.g., tetrahedrons, voronoi cells, rectangular blocks) or cubic splines or wavelets that interpolate between grid values. In this class of tomography, the large number of model parameters necessitates the use of iterative solvers such as *LSQR* [*Paige and Saunders*, 1982; *Nolet*, 1985] or *SIRT* [*Humphreys and Clayton*, 1988], with solution selection and resolution assessment less elegant than for direct inversions, but regularization (damping) can be used to avoid artifacts in regions of limited data coverage [*Spakman and Nolet*, 1988]. In the past decade the cell size used in regular grid inversions has decreased from about 6°x6° [*Inoue et al.*, 1990; *Pulliam et al.*, 1993] to 2°x2° [*Van der Hilst et al.*, 1997]. Plate 1b depicts *S* wavespeed variations in constant slowness blocks of 2.5°x2.5°x200km [*Grand, personal communication*, 1999; see *Grand et al.*, 1997], and Plate 1c depicts lateral variations in *P* wavespeed [*Kárason and Van der Hilst*, 2000] in 3°x3°x150km blocks. These map views reveal long linear features of faster-than-average wave propagation that reflect past episodes of plate convergence at Earth's surface. Even though the wavespeed variations may at first seem rather different, many structures in Plate 1a resemble the low-pass filtered version of those in Plates 1b and 1c, and if one considers the difference in nominal resolution the three models are, in fact, fairly consistent with each other in regions of adequate data coverage.

Flexible parameterization

Uneven source and receiver distribution results in significant spatial variations in data coverage. Global basis functions offer no flexibility for regionalization but a local basis can be adapted to lateral variations in data coverage. Small blocks can be used in densely sampled regions without unnecessary overparameterization of poorly sampled regions [e.g., *Bijwaard et al.*, 1998]. Ideally such irregular grids reflect the spatial variation of resolution, but since this is difficult to quantify they have been designed on the basis of sampling [*Gudmundsson and Sambridge*, 1998;

Bijwaard et al., 1998] or regional interest [*Abers and Roecker*, 1991; *Widiyantoro and Van der Hilst*, 1996]. Plate 2 illustrates the effect of different parameterizations.

Data quality and coverage

The success of any tomographic study depends critically on data quality. Most shear wave studies have been based on waveform data that were carefully selected and processed by individual investigators [e.g., *Woodhouse and Dziewonski*, 1984; *Masters et al.*, 1996; *Li and Romanowicz*, 1996; *Grand et al.*, 1997; *Van Heijst and Woodhouse*, 1999; *Ekström*, this volume; *Mégnin and Romanowicz*, this volume], but for global *P*-wave inversions such data sets are only now being constructed. With almost 15 million entries, the largest single data source available for tomography consists of the travel-time residuals processed and published by the International Seismological Centre (ISC). This data set is noisy but its size and redundancy allows the extraction of structural signal. Many researchers have processed the ISC data prior to inversion, but probably the most rigorous effort was made by *Engdahl et al.* [1998]. Using non-linear procedures for earthquake relocation and seismic phase re-identification they improved hypocenter parameters and travel time residuals for a large range of seismic phases. The striking agreement between images based either on travel times inferred from careful waveform processing (Plate 1b) or from routinely reported and processed phase arrivals (Plate 1c) demonstrates the value of the data processing by Engdahl and co-workers. It also demonstrates that — at least at the depth shown — compressional and shear wavespeed are highly correlated with each other.

Uneven data coverage continues to be one of the most persistent problems in travel time tomography, although the use of irregular grids can reduce some of its detrimental effects on imaging. For a given source-receiver distribution the sampling of Earth's structure can be improved by considering data and ray paths not only of direct *P* or *S* but of other phases as well. For *P*-wave imaging, seismologists have experimented successfully with depth phases (such as *pP*), which also helps constraining focal depth [*Engdahl et al.*, 1998], surface reflections (such as *PP* and *PPP*), and core reflected (*PcP*) and refracted (*PKP*) waves [cf. *Van der Hilst et al.*, 1991; *Van der Hilst and Engdahl*, 1991; *Obayashi and Fukao*, 1997; *Vasco and Johnson*, 1998; *Bolton and Masters*, 1998; *Van Heijst and Woodhouse*, 1999]. For *S* travel time tomography, arrival times of direct *S*, the multiple surface reflections such as *SS*, *SSS*, *SSSS*, core reflections and refractions *ScS*, *SKS*, and surface (Love) wave phase velocities have been used [cf., *Grand*, 1994; *Liu and Dziewonski*, 1998; *Widiyantoro et al.*, 1998]. Large gaps in data coverage remain, however. In regions where mantle structure cannot yet be resolved by body wave data one can impose zero perturbations from the reference model or use independent constraints on long wavelength variations, such as frequency shifts of Earth's free oscillations [*Kárason and Van der Hilst*, 1998; *Ishii and Tromp*, 1999].

A new model for mantle P-*wavespeed*

Because of our interest in the deep mantle [*Van der Hilst and Kárason*, 1999; *Kellogg et al.*, 1999], we made an effort to improve the sampling of lower mantle structure by incorporation of travel time data of core refracted *PKP* and diffracted P_{diff} waves [*Kárason and Van der Hilst*, 2000]. Figure 1 illustrates the ray geometry for these phases (NB. we used 3-D sensitivity kernels based on calculations by *Zhao et al.* [2000] for the back projection of the P_{diff} data but those are not shown here). In fact, we used differential times PKP_{DF}-PKP_{AB}, PKP_{BC}-PKP_{AB}, and PKP_{DF}-P_{diff} to reduce effects of hypocenter mislocation and to facilitate the extraction of signal from structure in the deep mantle. Moreover, the requirement that several readings be made from a single record works as an excellent quality criterion [*Kárason and Van der Hilst*, 2000]. For these phases we used accurate travel times inferred from waveform cross correlation by *McSweeney* [1997] (1383 *PKP* differential times) and *Wysession* [1996] (542 P_{diff} differential times) as well as some 27,412 carefully selected and processed *PKP* differential data from the data base of Engdahl and co-workers. These data were used along with nearly 8 million *P* and *pP* data from the Engdahl catalog; see *Kárason and Van der Hilst* [2000] for details about the data integration. This augmented data set provides much better data coverage than the *P* data alone (Figure 2), in particular in the southern hemisphere.

Plate 3 illustrates how the lateral variation of *P*-wavespeed changes with increasing depth in the mantle. The signature of cratonic parts of ancient continents and the narrow linear anomalies associated with plate subduction characterize structure in the upper mantle. (We remark that in this model the thickness of continental lithosphere is not well resolved since for most continental receivers these the body waves used sample shallow mantle structure in only a small range of incident angles.) In the mid-mantle the amplitude of wavespeed variations is significantly smaller than in the upper mantle, but a pattern of long, tabular structural features emerges beneath the major convergent plate boundaries (see also Plate 1). The thickness of these tabular structures is much larger than the subducted slabs in the shallow mantle, which can perhaps be attributed to radial changes in viscosity [*Fischer et al.*, 1990; *Bunge et al.*, 1996]. Toward the base of the mantle

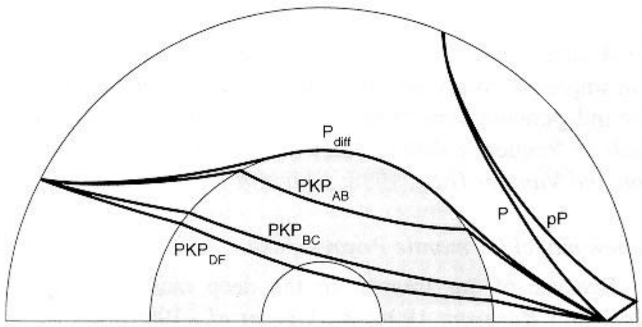

Figure 1. Ray geometry for the phases used in the *P*-wave study by Kárason and Van der Hilst [2000]. The core refracted *PKP* and diffracted P_{diff} waves provide better sampling of the deep mantle than *P* waves alone. We remark that instead of narrow rays we used 3-D sensitivity kernels to account for the fact that the P_{diff} travel times were measured from long period waveforms [*Wysession*, 1996]. The sensitivity kernels were based on mode summation [*Zhao et al.*, 1999].

the peak-to-peak amplitudes increase, albeit not as much as reported for shear wave perturbations [*Masters et al.*, 1996]. Figure 3 depicts an estimate of spatial resolution at selected depths. As expected from the uneven data coverage, the image recovery also reveals large geographical variations, but the changes in the character of heterogeneity from mid-mantle to the base of the mantle can not be attributed to sampling alone. The detail provided by the fine parameterization in regions of dense sampling is lost in the global maps of Plate 3 and Figure 3 but can be appreciated once we zoom into a particular region (Plate 2) or display structure by means of vertical sections across selected plate margins (Plate 4).

RESULTS OF IMAGING PERTINENT TO THE ISSUE OF MANTLE CONVECTION

While many early results [*Dziewonski*, 1984; *Woodhouse and Dziewonski*, 1984] have proved to be robust, long wavelength models continue to be improved, and in recent studies the wavespeed variations are expanded up to l=24 [*Ekström*, this issue; *Mégnin and Romanowicz*, this issue]. This class of modeling does not, however, resolve trajectories of mantle flow in sufficient detail to determine unequivocally whether or not convection is stratified at 660 km. Indeed, its results can be used to argue either way [*Richards and Engebretson*, 1992; *Wen and Anderson*, 1995]. In the 1990's, travel time tomography with local basis functions has made several seminal contributions to our understanding of mantle convection because it has enabled the mapping of flow trajectories in unprecedented detail.

First, some slabs of subducted lithosphere penetrate into the lower mantle while others appear trapped in the upper mantle. This was first borne out by regional studies [e.g., *Zhou and Clayton*, 1990; *Van der Hilst et al.*, 1991; *Fukao et al.*, 1992] but has since been confirmed by other studies, including high resolution global inversions [*Widiyantoro*, 1997; *Bijwaard et al.*, 1998; *Kárason and Van der Hilst*, 1999]. Plate 4 provides examples of both styles of subduction. Slab deflection may occur beneath Izu Bonin and the southern Kuriles (Plate 4b,c), the Banda arc, and beneath the Thyrrenian Sea; deep slabs, sometimes severely deformed in the transition zone, have been detected beneath the Mariana, Tonga-Kermadec (Plate 4e), Sunda (4d), and northern Kurile arcs, the Philippines, the Aegean Sea (4a), and Central and South America (4f). Inspired by *Kincaid and Olson* [1987], *Van der Hilst and Seno* [1993] and *Van der Hilst* [1995] argued that the observed complexity does

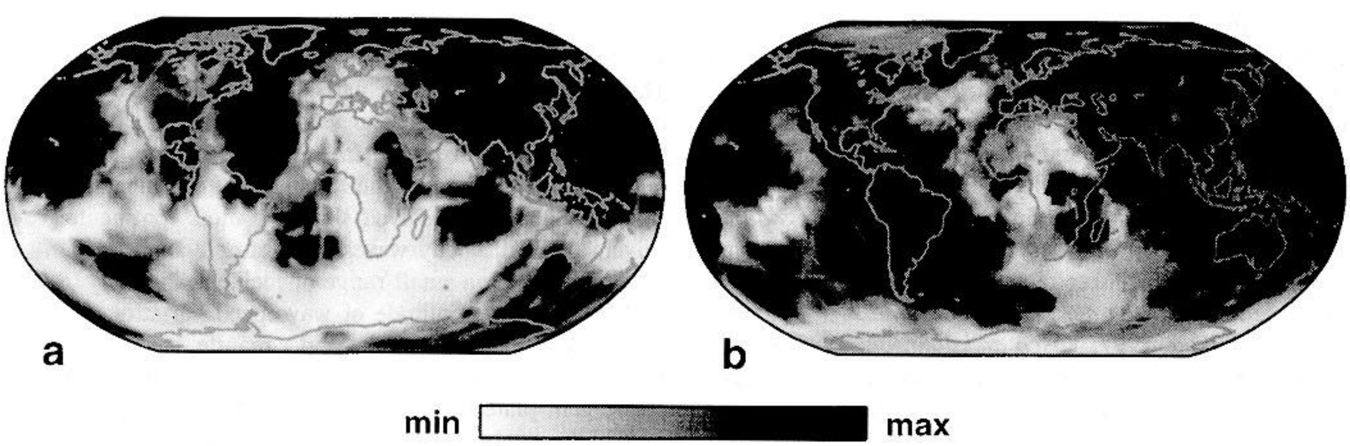

Figure 2. Improvement of sampling of deep mantle structure: (a) sampling by *P* and *pP* and (b) *PKP* and P_{diff}. Shown here are the column sums of the sensitivity matrix **A** used by *Kárason and Van der Hilst* [2000].

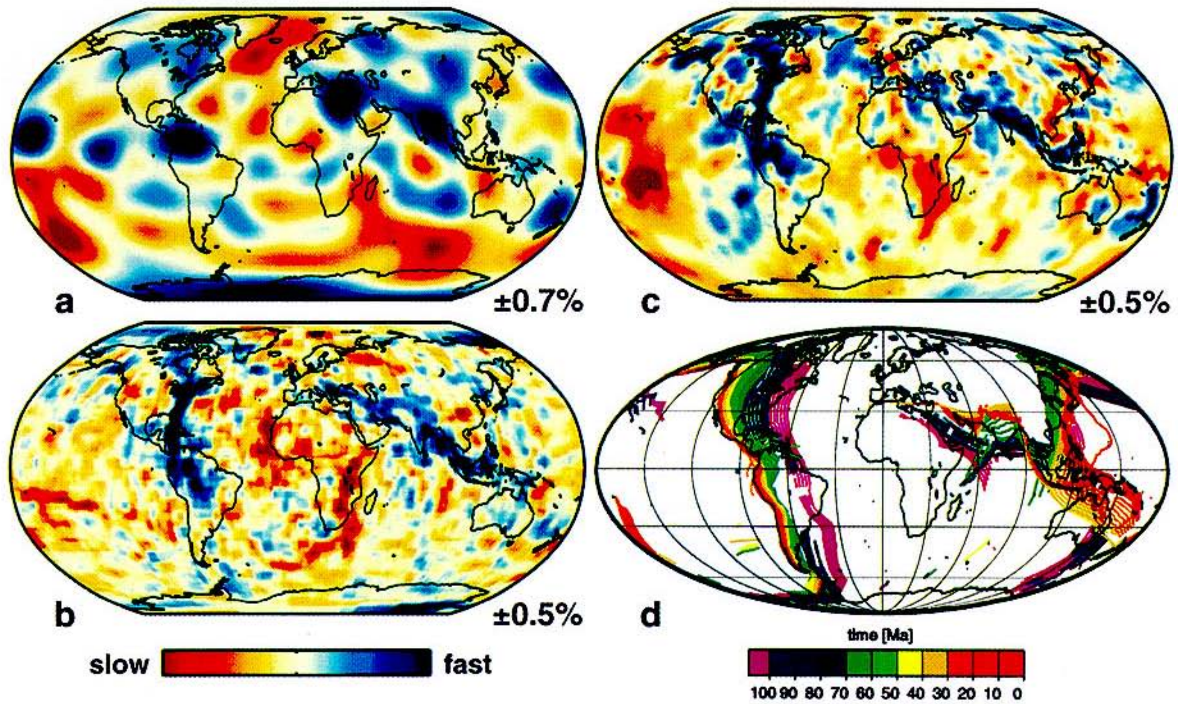

Plate 1. Robinson projections of lateral variation of seismic wavespeed at approximately 1300 km depth. (a) *S* wavespeed expanded on global basis functions (spherical harmonics up to degree and order 12) by *Su et al.* [1994]; (b) *S* wavespeed represented by regular blocks as local basis functions [*Grand, personal communication*, 1999; see *Grand et al.*, 1997]; (c) *P* wavespeed represented by blocks [Kárason and Van der Hilst, 2000]. The relative amplitude of the perturbations is given at the bottom right of each panel. (d) Mollweide projection of the history of plate convergence [cf. *Lithgow-Bertelloni and Richards*, 1998]; color indicates time interval in which subduction occurred.

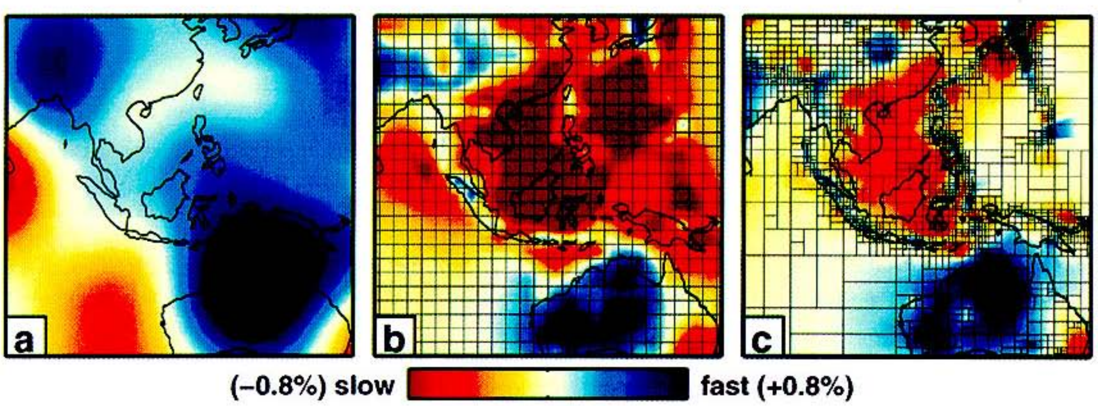

Plate 2. Lateral variation in seismic wavespeed at about 300 km depth beneath Australiasia according to different global models published in the last decade. (a) Spherical harmonics up to degree and order 12 [*Su et al.*, 1994]; (b) *P* wavespeed on a regular 3°x3° grid [*Kárason and Van der Hilst*, 2000]; (c) *P* wavespeed on an irregular grid [*Kárason and Van der Hilst*, 1999]. The image based on spherical harmonics is dominated by the high wavespeeds of the continental cratons in Australia and central Asia, and in the regular grid inversion the signature of the narrow slabs is overwhelmed by the low wavespeed in the back arc regions. Irregular gridding [e.g., *Bijwaard et al.*, 1998; *Kárason and Van der Hilst*, 1999] gives the most satisfactory rendering of the actual structure. Results similar to Plate 2c can be obtained by using small cells in a regular grid inversions [e.g., *Widiyantoro and Van der Hilst*, 1996] but for global inversions the number of model parameters would then become very large.

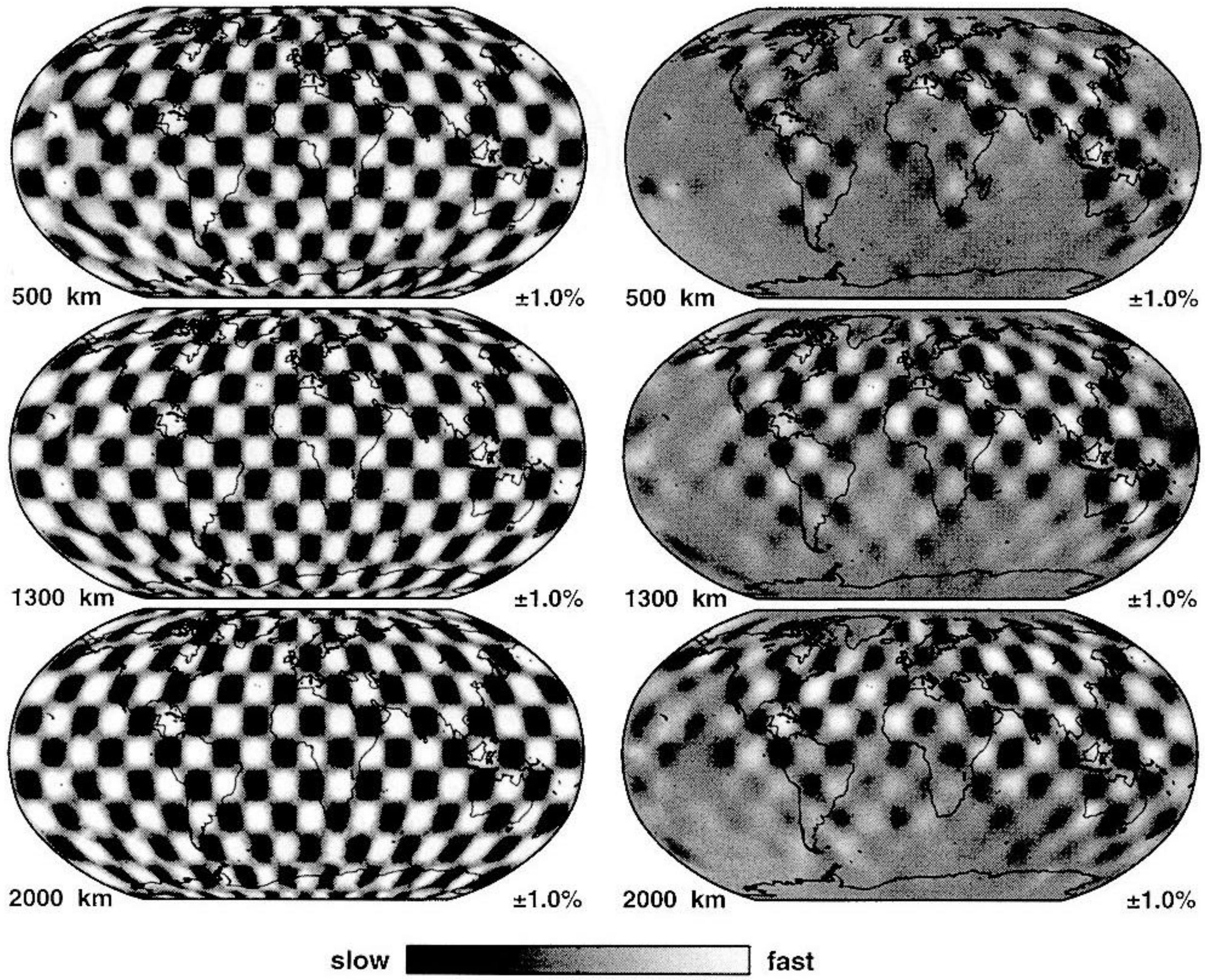

Figure 3. Estimate of spatial resolution at 500, 1300, and 2000 km depth. From the input model shown on the left we calculated synthetic travel time residuals by ray tracing and we then inverted them to test if (and where) we can resolve the know input pattern with the data coverage used. The input anomaly is ±2% in the center of each cell. This exercise shows that there are large regions in the mantle were resolution is poor owing to inadequate sampling, in particular in the upper mantle. Notice also that image recovery at 2000 km depth is equal to or better than at 1300 km, which indicates that the dramatic change in heterogeneity, compare, for instance, Plates 3d and e, is not simply related to sampling.

not imply stratification at 660 km depth but can be caused by interplay between relative plate motion (i.e., lateral trench migration) and the deformation of slabs when they encounter resistance (e.g., higher viscosity or a depressed phase boundary). Experimental [*Griffiths et al.*, 1995; *Guiltier-Frottier et al.*, 1995] and numerical [*Zhong and Gurnis*, 1995; *Davies*, 1995; *Christensen*, 1996] fluid dynamical experiments support this view, but selective weakening of the descending plate by grainsize reduction upon phase transformation may also contribute [*Riedel and Karato*, 1997]. The complexity caused by interaction of downwellings with the upper mantle transition zone persists to near 1000 km depth [*Van der Hilst and Kárason*, 1999] but the significance of this depth is not yet established and many slabs sink to even larger depth (Plate 4).

Second, independent *P* and *S* studies have begun to agree on structure as small as several hundred km [*Grand et al.*, 1997; *Van der Hilst et al.*, 1997] - a development that has increased the credibility of this class of imaging and may prove to be one of the milestones of tomography;

they revealed a relatively simple pattern of narrow high-wavespeed structures in the lower mantle beneath plate boundaries with a long history of subduction (Plate 1) and indicated that these deep structures often connect to seismogenic slabs in the upper mantle (Plate 4). Several slab structures disappear from tomographic view in the bottom 1000 km of the mantle (e.g., Plates 4a, d-f), but some fragments seem to connect to D" heterogeneity, for instance beneath eastern Asia and central America. Also the correlation between *P* and *S* images, which persists to large depth, may break down near the base of the mantle [*Grand et al.*, 1997; *Su and Dziewonski*, 1997; *Kennett et al.*, 1998].

Third, despite theoretical and practical difficulties significant progress has been made in the mapping of seismically slow anomalies, and several studies now suggest that mantle upwellings are continuous over a large depth range, supporting the view that 'plumes' originate (at a boundary layer) below the 660 km discontinuity [*Wolfe et al.*, 1997; *Bijwaard and Spakman*, 1999; *Goes et al.*, 1999; *Ritsema et al.*, 1999]. Image resolution — in particular in the radial direction — continues to form a formidable obstacle, however.

SCALE OF MANTLE CONVECTION

These observations render untenable the conventional end-member views of either convective stratification at 660 km or undisturbed whole mantle flow. The 660 km discontinuity distorts mantle flow, occasionally resulting in local and transient layering, but many slabs penetrate to at least 1700 km depth in the mantle. The change in structure and heterogeneity spectrum between 1700 and 2300 km depth is probably real, but its origin is not yet known. It may point to stratification of some sort in the deep mantle [*Van der Hilst and Kárason*, 1999; *Kellogg et al.*, 1999], but it may also reflect changes in the nature of global plate motion in the distant past [*Richards and Engebretson*, 1992]. Alternatively, *Anderson* [1999] explains the slab-like lower mantle structures and their apparent continuity to upper mantle subduction zones by thermal coupling and coincidental alignment of structures in separately convecting upper and lower mantles. We take issue with this. It would be very fortuitous indeed if slowly changing structures in the sluggish lower mantle align with rapidly changing structures in the less viscous upper mantle. Thermal coupling can work [*Nataf*, 1988; *Čížková et al.*, 1999] but is too slow to explain the large depth of slab penetration beneath young convergent margins and is inconsistent with the constant dip angle inferred for several slabs. Moreover, if only heat is exchanged, thousands of kilometers of subducted lithosphere must have accumulated in the upper mantle beneath margins with a long subduction record, for which there is no observational evidence.

The geophysical evidence against stratification at 660 km depth is strong, and if isolated and seismically visible 'reservoirs' exist they are likely to reside at a larger depth. A mantle convection scenario that is then worth considering is one in which — apart from the upper and lower boundary layers (lithosphere and D", respectively) — three domains are identified. In the view postulated by *Kellogg et al.* [1999] and *Van der Hilst and Kárason* [1999], and discussed by *Albarède and Van der Hilst* [1999], undegassed and enriched material in the bottom 1000 km of the mantle has not (yet) mixed with the part of the mantle — the top 2000 km or so — that is involved in the recycling of slab material, has a relatively uniform major element composition, and represents the depleted and outgassed source of mid-ocean ridge basalts. The upper mantle transition zone (400-1000 km depth) divides the depleted part of the mantle in a well mixed, low viscosity domain and a deeper one with high viscosity and slower transients; here, mantle flow is distorted by viscosity stratification, effects of phase transitions in the mantle silicates, and changes in plate motion at Earth's surface.

For long term survival the deep domain must have a slightly higher intrinsic density than the overlying depleted mantle [*Tackley*, 1998; *Kellogg et al.*, 1999]. The interface between these domains would be close to isopycnic (i.e., compositional and thermal effects on buoyancy are in balance) and significant dynamic topography can develop with some slabs penetrating to near the CMB [*Kellogg et al.*, 1999]; this resembles the 'penetrative' convection proposed previously for stratification at 660 km depth [*Silver et al.*, 1988]. The anomalous deep mantle "layer" — if it indeed exists — could represent long-lived differences in composition or phase chemistry [*Van der Hilst and Kárason*, 1999]. Alternatively, in an evolutionary sense, it may not yet have been churned by subduction. It takes many tens of millions of years (or more) before changes in the plate configuration at Earth's surface affect the heterogeneity structure of the deep mantle. Moreover, as cold slabs sink, their negative buoyancy can be diminished (or enhanced) by phase reactions in the upper mantle transition zone and may be neutralized by compositional effects well above the very base of the mantle [*Kesson et al.*, 1998]. In this transient system recycling may involve only the upper and mid-mantle, and few subduction systems may have operated long enough to produce (sufficiently 'cold') slabs that reach the CMB and churn the deep layer. This can be tested by rigorous integration of plate reconstructions and tomographic images of mantle structure [*Besse, personal communication*, 1999] by means of numerical modeling [e.g., *Bunge et al.*, 1998].

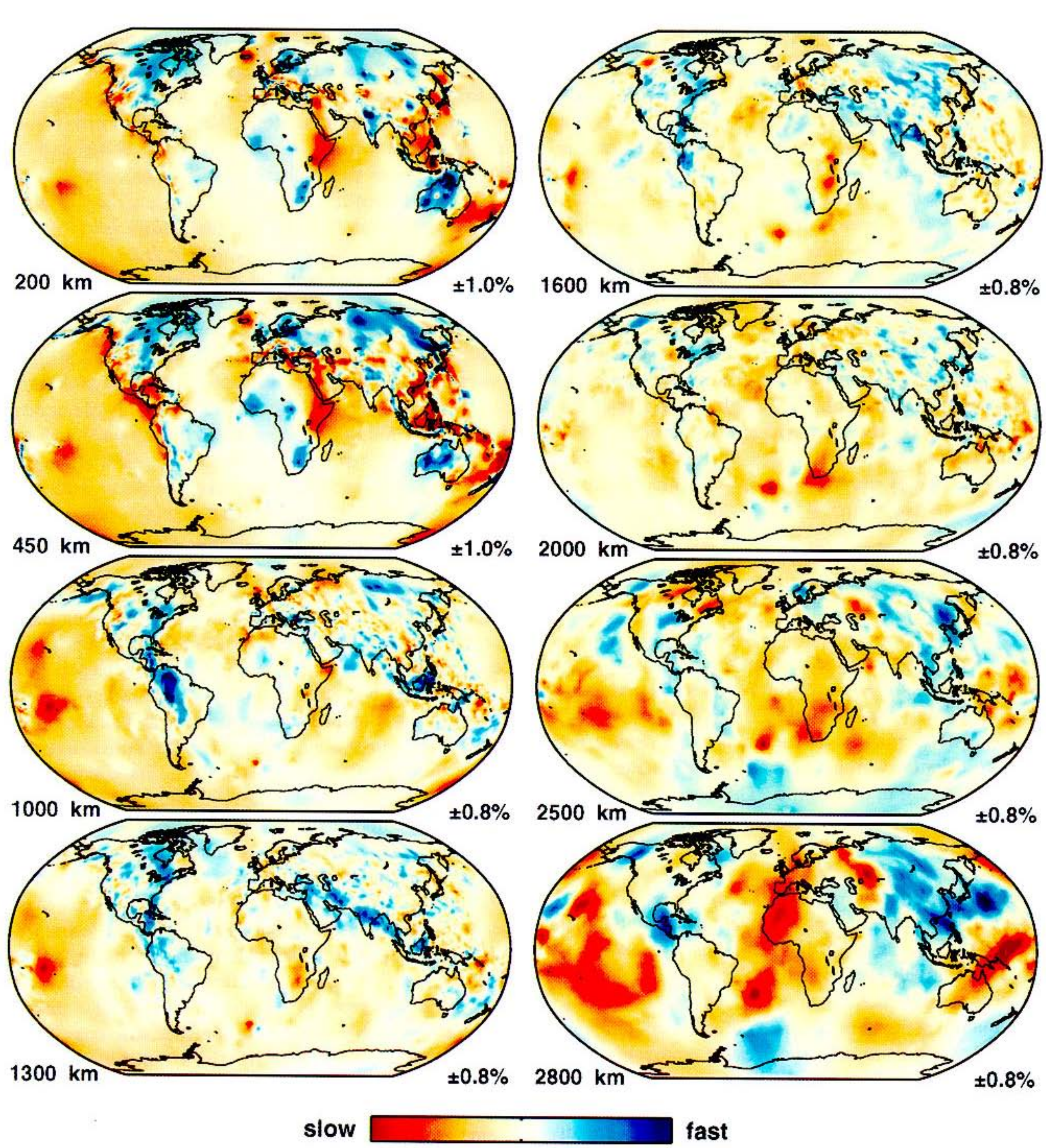

Plate 3. Robinson projections of the lateral variation in P wavespeed at several depths in Earth's mantle according to *Kárason and Van der Hilst* [1999]. This model is based on data from the seismic phases displayed in Figure 1, and thus benefits from improved sampling in the deep mantle (Figure 2), and the flexible parameterization illustrated in Plate 2 (although the effect of the irregular grid is hardly appreciated at this scale).

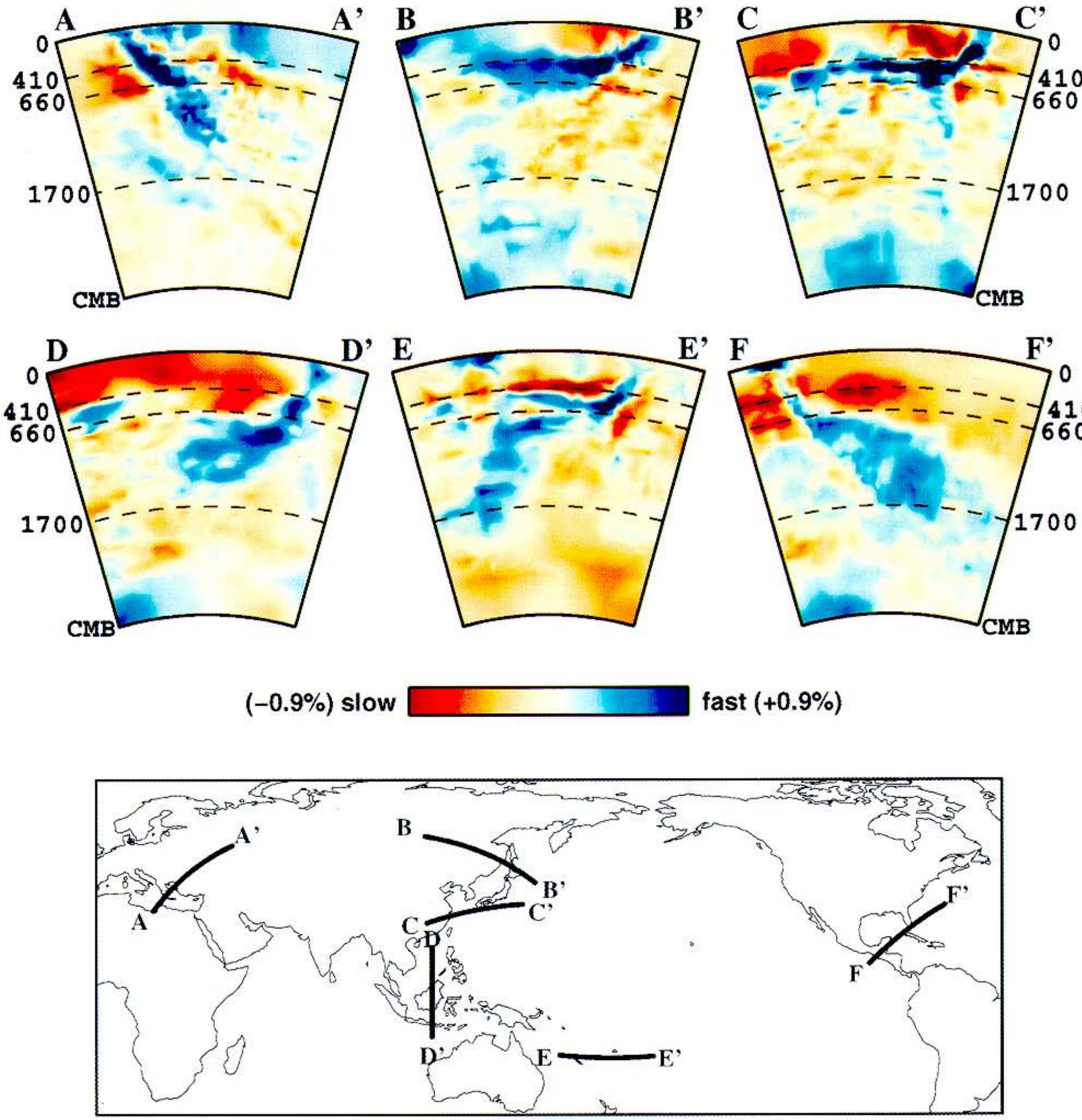

Plate 4. Slab structure illustrated by vertical mantle sections across (a) the Hellenic (Aegean), (b) southern Kurile, (c) Izu Bonin, (d) Sunda (Java), and (e) the northern Tonga island arcs, and (f) central America. See map inset for cross section locations.

DIRECTIONS FOR FUTURE RESEARCH

Seismic tomography did not settle the debate about the scale of mantle convection just by demonstrating the deep penetration of many slabs, but it has moved research away from conventional — but inadequate — end-member convection models. Many aspects of mantle convection remain enigmatic [e.g., *Albarède and Van der Hilst*, 1999]. Seismic imaging will continue to play a central role in constraining the pattern of convective flow, but several issues must be sorted out. However dramatic the "red-and-blue" images, our actual understanding of them is unsatisfactory. We need better constraints on the amplitude of the changes in P and S-wavespeed, and their ratio $\delta lnV_S/\delta lnV_P$, and we need to integrate them with results from experimental and theoretical mineral physics to quantify changes in temperature, phase, and bulk composition. In addition, the trajectories of mantle convection must be delineated in even more detail in order to resolve outstanding issues, such as the ultimate fate of the slabs that penetrate across the upper mantle transition zone and the source and morphology of the return flow (plumes?). The latter requires a significant effort to improve data coverage beneath regions far away from seismically active plate boundaries. Seismic anisotropy can also be used as a tool for delineating flow trajectories [*Montagner*, 1998]. Continued imaging of mantle structure beneath convergent margins and better integration with the record of plate motions through computational geodynamic modeling will further our understanding of subduction and its partnership with mantle convection.

Acknowledgments. We thank Wei-jia Su and Steve Grand for providing us with their models, Li Zhao for the mode calculations that we used to approximate the sensitivity kernels for the PKP_{DF}-P_{diff} travel time differentials, Bernard Steinberger for producing the diagram used as Plate 1d, and Mark Richards and Richard Gordon for constructive reviews. This research is supported by the National Science Foundation (EAR-9909492).

REFERENCES

Abers, G.G., and S.W. Roecker, Deep structure of an arc-continent collision: Earthquake relocation and inversion for upper mantle P and S velocities beneath Papua New Guinea, *J. Geophys. Res.*, 96, 6379-6401, 1991.

Aki, K.A., A. Christoffersson, and E.S. Husebye, Determination of the three-dimensional seismic structure of the lithosphere, *Geophys. J. R. astron. Soc.*, 82, 277-296, 1977.

Albarède, F., and R.D. van der Hilst, New mantle convection model may reconcile conflicting evidence, *EOS Trans. Am. Geophys. Un.*, 45, 535-539, 1999.

Anderson, D.L., Tomography, Gutenberg, and Freud: are color cross sections really Rorschach tests? *EOS Trans. Am. Geophys. Un.*, 80, F719, 1999

Bijwaard, H. and W. Spakman, Tomographic evidence for a narrow whole mantle plume below Iceland, *Earth Planet. Sci. Lett.*, 166, 121-126, 1999.

Bijwaard, H., W. Spakman, and E.R. Engdahl, Closing the gap between regional and global travel time tomography, *J. Geophys. Res.*, 103, 30055-30078, 1998.

Boschi, L., and A.M. Dziewonski, High- and low resolution images of Earth's mantle: implication of different approaches to tomographic modeling, *J. Geophys. Res.*, 104, 25567-25594, 1999.

Bunge, H.-P., M.A. Richards, and J.R. Baumgardner, The effect of viscosity stratification on mantle convection, *Nature*, 379, 436-438, 1996.

Bunge, H.-P., Richards, M.A., Lithgow-Bertelloni, C., Baumgardner, J.R., Grand, S.P., and Romanowicz, B.A., Time scales and heterogeneous structure in geodynamic Earth models, *Science*, 280, 91-95, 1998.

Christensen, U.R., The influence of trench migration on slab penetration into the lower mantle, *Earth Planet. Sci. Lett.*, 140, 27-39, 1996.

Čížková, H., O. Čadek, A.P. van den Berg, and N.J. Vlaar, Can lower mantle slab-like anomalies be explained by thermal coupling between the upper and lower mantles? *Geophys. Res. Lett.*, 26, 1501-1504, 1999.

Davies, G.F., Penetration of plates and plumes through the mantle transition zone, *Earth Planet. Sci. Lett.*, 133, 507-516, 1995.

Dziewonski, A.M., B.H. Hager, and R.J. O'Connell, Large-scale heterogeneities in the lower mantle, *J. Geophys. Res.*, 82, 239-255, 1977.

Dziewonski, A.M., Mapping the lower mantle: determination of lateral heterogeneity up to degree and order 6, *J. Geophys. Res.*, 89, 5929-5952, 1984.

Engdahl, E.R., R.D. van der Hilst, and R. Buland, Global teleseismic earthquake relocation with improved travel times and procedures for depth determination, *Bull. Seism. Soc. Am.*, 88, 722-743, 1998.

Fischer, K., T.H. Jordan, and K.C. Creager, Seismic constraints on the morphology of deep slabs, *J. Geophys. Res.*, 93, 4773-4783, 1988.

Fukao, Y., M. Obayashi, H. Inoue, and M. Nenbai, Subducting slabs stagnant in the mantle transition zone, *J. Geophys. Res.*, 97, 4809-4822, 1992.

Goes, S., W. Spakman, and H. Bijwaard, A lower mantle source for central European volcanism, *Science*, 286, 1928-1931, 1999.

Grand, S.P., Mantle shear structure beneath the Americas and surrounding oceans, *J. Geophys. Res.* 99, 11,591-11,621, 1994.

Grand, S.P., R.D. van der Hilst, and S. Widiyantoro, Global seismic tomography: A snapshot of convection in the Earth, *Geol. Soc. Am. Today*, 7, No. 4, 1-7, 1997.

Griffiths, R.W., R.I. Hackney, and R.D. van der Hilst, A laboratory investigation of effects of trench migration on the descent of subducted slabs, *Earth Planet. Sci. Lett.*, 133, 1-17, 1995.

Guillou-Frottier, L., J. Buttles, and P. Olson, Laboratory experiments of the structure of subducted lithosphere, *Earth Planet. Sci. Lett.*, 133, 19-34, 1995.

Gudmundsson, O., and M. Sambridge, A regionalized upper mantle (RUM) seismic model, *J. Geophys. Res.*, 103, 7121-7130, 1998.

Humphreys, E., and R.W. Clayton, Adaption of backprojection tomography to seismic travel time problems, *J. Geophys. Res.*, 93, 1073-1085, 1988.

Inoue, H., Y. Fukao, K. Tanabe, and Y. Ogata, Whole mantle *P*-wave travel time tomography, *Phys. Earth Planet. Inter.*, 59, 294-328, 1990.

Ishii, M. and J. Tromp, Normal-mode and free-air gravity constraints on lateral variations in velocity and density of Earth's mantle, *Science*, 285, 1231-1236, 1999.

Julian, B.R., and M.K. Sengupta, Seismic travel time evidence for lateral inhomogeneity in the deep mantle, *Nature*, 242, 443-447, 1993.

Kárason, H., and R.D. van der Hilst, Improving seismic models of whole mantle *P*-wavespeed by the inclusion of data from differential times and normal modes, *EOS Trans. Am. Geoph. Un.*, 79, F656, 1998.

Kárason, H., and R.D. van der Hilst, New constraints on 3D variations in mantle *P* wavespeed, *EOS Trans. Am. Geoph. Un.*, 80, F731, 1999.

Kárason, H., and R.D. van der Hilst, Improving global tomography models of P-wavespeed I: Incorporation of differential times of refracted and diffracted core phases (*PKP, Pdiff*), *J. Geophys. Res.* (under review), 2000.

Kellogg, L.H., B.H. Hager, and R.D. van der Hilst, Compositional stratification in the deep mantle, *Science*, 283, 1881-1884, 1999.

Kennett, B.L.N., S. Widiyantoro, and R.D. van der Hilst, Joint seismic tomography for bulk-sound and shear wavespeed, *J. Geophys. Res.*, 103, 12469-12493, 1998.

Kesson, S.E., J.D. Fitz Gerald, and J.M. Shelley, Mineralogy and dynamics of a pyrolite lower mantle, *Nature*, 397, 252-255, 1998.

Kincaid, C. and P. Olson, An experimental study of subduction and slab migration, *J. Geophys. Res.*, 92, 13832-13840, 1987.

Li, X.-D. and B. Romanowicz, Global mantle shear-velocity model developed using nonlinear asymptotic coupling theory, *J. Geophys. Res.*, 101, 22245-22272, 1996.

Lithgow-Bertelloni, C. and M. Richards, The dynamics of Cenozoic and Mesozoic plate motions, *Rev. Geophys.*, 36, 27-78, 1998.

Liu, X.-F., and A.M. Dziewonski, Global analysis of shear wave velocity anomalies in the lower-most mantle, In: *Observational and theoretical constraints on the Core Mantle Boundary Region*, Gurnis, M., Wysession, M.E., Knittle, E., and Buffett, B.A. (Eds.), Geodynamics Series (American Geophysical Union), 28, 21-36, 1998.

Masters, G., S. Johnson, G. Laske, and H. Bolton, A shear-velocity model of the mantle, *Phil. Trans. R. Soc. Lond. A*, 354, 1385-1411, 1996.

McSweeney, T., *PhD thesis*, (supervisor K.C. Creager) University of Washington, Seattle, 1997.

Montagner, J.-P., Can seismic tomography tell us anything about convection in the mantle? *Rev. Geophys.*, 32, 115-137, 1994.

Montagner, J.-P., Where can seismic anisotropy be detected in Earth's mantle? In boundary layers ...., *Pure Appl. Geophys.*, 151, 223-156, 1998.

Nataf, H.-C., What is responsible for thermal coupling in layered convection? *J. Phys - Paris*, 49, 1707-1714, 1988.

Nolet, G., Solving or resolving inadequate and noisy tomographic system, *J. Comp. Phys.*, 61, 463-482, 1985.

Obayashi, M., and Y. Fukao, *P* and *PcP* travel time tomography for the core-mantle boundary, *J. Geophys. Res.*, 102, 17825-17842, 1997.

Paige, C. C., and M. A. Saunders, LSQR: an algorithm for sparse linear equations and sparse least squares, ACM Trans.Math.Soft., 8, 43-71 and 195-209, 1982.

Pulliam, R.J., Vasco, D.W. and Johnson, L.R., Tomographic inversions for mantle P-wave velocity structure based on the minimization of l^2 and l^1 norms of International Seismological Centre travel time residuals, *J. Geophys. Res.*, 98, 699-734, 1993.

Richards, M.A., and D.C. Engebretson, Large-scale mantle convection and the history of subduction, *Nature*, 355, 437-440, 1992.

Riedel, M.R., and S. Karato, Grain-size evolution in subducted oceanic lithosphere associated with the olivine-spinel transformation and its effects on rheology, *Earth Planet. Sci. Lett.*, 148, 27-43, 1997.

Ritsema, J., H.J. van Heijst, and J.H. Woodhouse, Complex shear wave velocity structure imaged beneath Africa and Iceland, *Science*, 286, 1925-1928, 1999.

Ritzwoller, M., and E.M. Lavely, 3-dimensional models of Earth's mantle, *Rev. Geophys.*, 33, 1-66, 1995.

Romanowicz, B., Seismic tomography of Earth's mantle, *Ann. Rev. Earth Planet. Sci.*, 19, 77-99, 1991.

Sengupta, M.K., and M.N. Toksöz, Three-dimensional model of seismic velocity variations in the earth's mantle, *Geophys. Res. Lett.*, 3, 84-86, 1976.

Silver, P.G., R.W. Carlson, and P. Olson, Deep slabs, geochemical heterogeneity, and the large-scale structure of mantle convection, *Ann. Rev. Earth Planet. Sci.*, 16, 477-541, 1988.

Spakman, W. and Nolet, G., Imaging algorithms, accuracy and resolution in delay time tomography, In: *Mathematical Geophysics: a Survey of Recent Developments in Seismology and Geodynamics,* pp. 155-188, ed. N.J. Vlaar *et al.*, Reidel, Dordrecht, 1988.

Su, W.-j., R.L. Woodward, and A.M. Dziewonski, Degree 12 model of shear velocity heterogeneity in the mantle, *J. Geophys. Res.*, 99, 6945-6981, 1994.

Su, W.-j., and A.M. Dziewonski, Simultaneous inversion for 3D variations in shear and bulk velocity in the mantle, *Phys. Earth Planet. Inter.*, 100, 135-156, 1997.

Van Heijst, H.J., and J.H. Woodhouse, Global high resolution phase velocity distributions of overtone and fundamental-mode surface waves determined by mode branch stripping, *Geophys. J. Int.*, 137, 601-620, 1999.

Van der Hilst, R.D., Complex morphology of subducted lithosphere in the mantle beneath the Tonga trench, *Nature*, 374, 154-157, 1995.

Van der Hilst, R.D., E.R. Engdahl, W. Spakman, and G. Nolet, Tomographic imaging of subducted lithosphere below northwest Pacific island arcs, *Nature*, 353, 37-43, 1991.

Van der Hilst, R.D., and T. Seno, Effects of relative plate motion on the deep structure and penetration depth of slabs below the Izu-Bonin and Mariana island arcs, *Earth Planet. Sci. Lett.*, 120, 395-407, 1993.

Van der Hilst, R.D., S. Widiyantoro, and E.R. Engdahl, Evidence for deep mantle circulation from global tomography, *Nature*, 386, 578-584, 1997.

Van der Hilst, R.D., and H. Kárason, Compositional heterogeneity in the bottom 1000 km of Earth's mantle: towards a hybrid convection model, *Science*, 283, 1885-1888, 1999.

Vasco, D.W., and L.R. Johnson, Whole earth structure estimated from seismic arrival times, *J. Geophys. Res.*, 103, 2633-2671, 1998.

Wen, L.X., and D.L. Anderson, The fate of slabs inferred from seismic tomography and 130 million years of subduction, *Earth Planet. Sci. Lett.*, 133, 185-198, 1995.

Widiyantoro, S., *Ph.D. Thesis*, (supervisors B.L.N. Kennett and R.D. van der Hilst) Australian National University, Canberra, Australia, 1997.

Widiyantoro, S., and R.D. van der Hilst, Structure and evolution of lithospheric slab beneath the Sunda arc, Indonesia, *Science*, 271, 1566-1570, 1996.

Widiyantoro, S., Kennett, B.L.N., and Van der Hilst, R.D., Extending shear-wave tomography for the lower mantle using S and SKS arrival-time data, *Earth, Planets, and Space*, 50, 999-1012, 1998.

Widiyantoro, S., Kennett, B.L.N., and Van der Hilst, R.D., Seismic tomography with P and S data reveals lateral variations in the rigidity of slabs, *Earth Planet. Sci. Lett.*, 173, 91-100, 1999.

Wolfe, C.J., I.Th. Bjarnason, J.C. VanDecar, and S.C. Solomon, Seismic structure of the Iceland mantle plume, *Nature*, 385, 245-247, 1997.

Woodhouse, J. H., and A.M. Dziewonski, 1984, Mapping the upper mantle: Three-Dimensional modeling of earth structure by inversion of seismic waveforms, *J. Geophys. Res.*, 89, 5953-5986, 1994.

Woodhouse, J.H. and A.M. Dziewonski, Seismic modeling of the Earth's large scale structure, *Phil. Trans. R. Soc. A.*, 328, 291-308, 1989.

Wysession, M.E., Continents of the core, *Nature*, 381, 373-374, 1996.

Zhao, L., T.H. Jordan, and C. Chapman, Three-dimensional Fréchet differential kernels, *Geophys. J. Int.* (in press) 2000.

Zhong, S. and M. Gurnis, Mantle convection with plates and mobile, faulted plate margins, *Science*, 267, 838-843, 1995.

Zhou, H.-w, and R.W. Clayton, *P* and *S* wave travel time inversions for subducting slabs under the island arcs of the northwest Pacific, *J. Geophys. Res.*, 95, 6829-6851, 1990.

H. Kárason and R. D. van der Hilst, Department of Earth, Atmospheric and Planetary Sciences, Massachusetts Institute of Technology, Cambridge, MA, 02139, USA.
(emails: karason@mit.edu, hilst@mit.edu)